Impact of the Channel Time-selectivity on BER Performance of Broadband Analog Network Coding with Two-slot Channel Estimation

Haris Gacanin†, Mika Salmela‡ and Fumiyuki Adachi§
†Motive Division, Alcatel-Lucent Bell N.V., Antwerp, Belgium
‡School of Science and Technology, Aalto University, Aalto, Finland
§Graduate School of Engineering, Tohoku University, Sendai, Japan
†Email: harisg@ieee.org

***Abstract*—Network coding at the physical layer (PNC) can be used to improve the network capacity in a wireless channel. Broadband analog network coding (ANC) was introduced as a simpler implementation of PNC. The coherent detection and self-information removal in ANC require accurate channel state information (CSI). In this paper, we theoretically investigate an impact of the channel time-selectivity on the bit error rate (BER) performance of broadband ANC with practical channel estimation (CE) scheme using orthogonal frequency division multiplexing (OFDM). The achievable BER performance gains due to the first and second order polynomial time-domain channel interpolation are evaluated using derived close-form BER expressions.**

***Index Terms*—Analog network coding, channel estimation, BER analysis, OFDM.**

I. Introduction

Recently, a physical-layer network coding (PNC) [1], [2] and analog network coding (ANC) [3]-[7] schemes have been proposed to increase the network capacity of bi-directional communication in a frequency-nonselective fading channel. On the other hand, in broadband wireless communications the channel is both time- and frequency-selective due to the user mobility and multipath propagation, respectively. These properties of the wireless channel render schemes in [1]-[7] not applicable for wireless communications. Thus, in [8], broadband ANC scheme was proposed for communication over a multipath (i.e., frequency-selective) channel.

The user mobility is an important factor in wireless communications that affects the bit error rate (BER) performance. Thus, a robust channel estimation (CE) is required to tract the fast fading variations. In broadband ANC scheme for coherent detection and self-information removal accurate CE is required. In [10], the BER performance of broadband ANC with pilot-assisted CE has been presented, but the tracking against the channel time-selectivity has not been investigated.

In this paper, we theoretically investigate the impact of channel time-selectivity on the BER performance of broadband ANC with two-slot pilot-assisted CE scheme in a frequency-selective fading channel. We present a closed-form BER expression based on orthogonal frequency division multiplexing (OFDM) radio access. We investigate the achievable BER performance gains in a fast-fading channel obtained by polynomial time-domain channel interpolation. Our analytical results shown that in a higher E_b/N_0 region the BER performance gains using pilot-assisted CE with both the first and second-order polynomial time-domain interpolation depend on the mobile user velocity.

The remainder of this paper is organized as follows. In Section II, we present the network model. The performance analysis is presented in Section III. In Section IV, the numerical results and discussions are presented. Finally, the paper is concluded in Section V.

II. Network Model

A bi-directional relay network with users U_0 and U_1, who are assumed to be out of each other's transmission range, and relay R is illustrated in Fig. 1. The transmission frame structure is illustrated in Fig. 2. The communication between two users in the mth block takes place during two slots; (i) in the first slot ($q = 0$) the users simultaneously transmit to the relay (ii) during the second slot ($q = 1$) the relay broadcasts the received signals to both users using an amplify-and-forward protocol. The figure shows that the kth frame consists of M blocks, where the first block ($m = 0$) is used for pilot-assisted CE.

A. Radio Access Scheme

The jth ($j \in \{0, 1\}$) user's mth block symbol sequence $\{d_{j,m}(n);\ n = 0 \sim N_c - 1,\ m = 0 \sim M - 1\}$ is fed to an N_c-point inverse fast Fourier transform (IFFT) to generate the jth user's time-domain OFDM signal in the $m$the frame (i.e., $s_{j,m}(t)$). Then, an N_g-sample guard interval (GI) is added and the GI-added OFDM signal is transmitted over a time-varying frequency-selective fading channel.

The propagation channel is characterized by the mth frame impulse response given by $h^k_{q,j,m}(\tau) = \sum_{l=0}^{L-1} h^k_{q,j,m}(l)\delta(\tau - \tau_l)$, where L denotes the number of paths, $h^k_{q,j,m}(l)$ denotes the path gain between the relay R and jth user U_j at slot q during the mth block of kth frame, $\delta(\cdot)$ denotes the delta function and τ_l denotes the time delay of the lth path. We

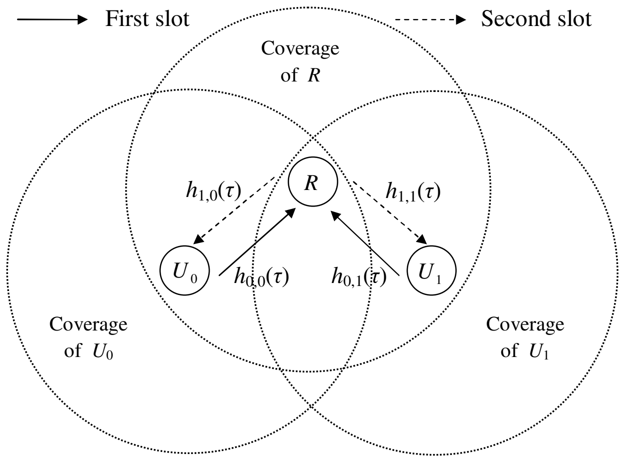

Fig. 1. Bi-directional relay network using ANC.

assume that the GI is assumed to be longer than the maximum channel time delay. The channel gain at the nth subcarrier is represented by $H^k_{q,j,m}(n) = FFT[h^k_{q,j,m}(\tau)]$. Henceforth we consider the mth block transmission and without loss of generality the frame index k can be omitted in the following.

First time slot: By assuming perfect time and frequency synchronization at the relay, during the first time slot (TS_0), the signals from both of the users T_0 and T_1 are transmitted to the relay terminal R. The received signal at the relay is amplified and broadcasted over a frequency-selective fading channel. For the sake of the analysis we normalize the transmit signal by a factor β, which is the square root of its noise variance.

Second time slot: During the second slot, by assuming perfect time and frequency synchronization, the received signal at the jth user U_j after FFT can be expressed as

$$R_{j,m}(n) = \frac{\sqrt{P}}{\beta}[\sqrt{P}d_{0,m}(n)H_{0,0,m}(n) + \sqrt{P}d_{1,m}(n)H_{0,1,m}(n) + N_{r,m}(n)]H_{1,j,m}(n) + N_{j,m}(n), \quad (1)$$

for $n = 0 \sim N_c - 1$, where $N_{j,m}(n)$ is the zero-mean noise having variance N_0/T_s due to the AWGN. The jth user U_j removes its self-information as

$$\tilde{R}_{j,m}(n) = R_{j,m}(n) - \frac{P}{\beta}d_{j,m}(n)H_{0,j,m}(n)H_{1,j,m}(n) \quad (2)$$

for $n = 0 \sim N_c - 1$. The decision variables are given by

$$\hat{d}_{j,m}(n) = \tilde{R}_{j,m}(n)w_{j,m}(n) \quad (3)$$

for $n = 0 \sim N_c - 1$, where $w_{j,m}(n)$ denotes the equalization weight [8].

B. Channel Estimation Scheme

The frame structure is illustrate in Fig. 2 with the kth frame divided into one pilot block and $M - 1$ data blocks. The channel estimates are obtained from the pilot signal, which is transmitted in the first block (i.e., $m = 0$) of the each frame. Blocks are divided into two stages, corresponding to the first and second time slot, TS_0 and TS_1, respectively, each consisting of $N_c + N_g$ samples (i.e., duration of T_s).

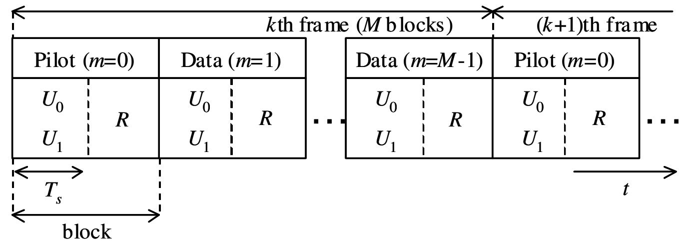

Fig. 2. Frame structure.

In the first time slot TS_0, the users U_0 and U_1, respectively transmit their pilot signals, $p_0(t)$ and $p_1(t) = p_0((t-\Delta)modN_c)$, where Δ denotes the time shift [10]. The relay estimates the channel gains and in the second time slot TS_1 broadcasts its pilot signal $p_0(t)$ to both users. Finally, the users estimate the corresponding channel gains using the broadcasted pilot signal in the first block. The estimated CSIs obtained from the pilot block are used in detecting the following $M - 1$ data blocks within the kth frame. For more details please refer to [10].

III. Performance Analysis

We first present the CE error model and then, we develop a closed-form BER expression with practical pilot-assisted CE scheme presented in [10], where the BER with perfect CSI is only presented as a reference.

A. CE Error Model

The estimated channel gains for the mth block within the kth frame can be represented as

$$\bar{H}^k_{q,j,m}(n) = H^k_{q,j,m}(n) + \epsilon^k_{q,j,m}(n) \quad (4)$$

for $n = 0 \sim N_c - 1$, where $\epsilon^k_{q,j,m}(n)$ is the channel estimation error. We model the channel estimation error ϵ as a zero-mean complex Gaussian random variable with the variance given by σ_e^2.

The decision variables after coherent detection in the mth OFDM data block given by (3) can be expressed as

$$\hat{d}_{j,m}(n) = X_{j,m}(n)Y^*_{j,m}(n), \quad (5)$$

for $n = 0 \sim N_c - 1$, where

$$\begin{cases} X_{j,m}(n) & = \frac{P}{\beta}d_{\bar{j},m}(n)H_{0,\bar{j},m}(n)H_{1,j,m}(n) \\ & + \frac{\sqrt{P}}{\beta}H_{1,j,m}(n)N_{r,m}(n) + N_{j,m}(n) \\ & + \frac{P}{\beta}d_{j,m}(n)H_{0,j,m}(n)H_{1,j,m}(n) \\ & - \frac{P}{\beta}d_{j,m}(n)H_{0,j,0}(n)H_{1,j,0}(n) \\ & - \frac{P}{\beta}d_{j,m}(n)H_{0,j,0}(n)\epsilon_{1,j,0}(n) \\ & + \epsilon_{0,j,0}(n)H_{1,j,0}(n) + \epsilon_{0,j,0}(n)\epsilon_{1,j,0}(n), \\ Y_{j,m}(n) & = H_{0,\bar{j},m}(n)H_{1,j,m}(n) + H_{0,\bar{j},0}(n)\epsilon_{1,j,0}(n) \\ & + \epsilon_{0,\bar{j},0}(n)H_{1,j,0}(n) + \epsilon_{0,\bar{j},0}(n)\epsilon_{1,j,0}(n). \end{cases} \quad (6)$$

Note that $\bar{c}$ represents the logical negation (i.e., NOT) of c. In the above expressions, we assume that for the given

$\{H_{q,j,m}(n)\}$ both $X_{j,m}(n)$ and $Y_{j,m}(n)$ are zero mean complex Gaussian random variables. Thus, the jth user's BER within the mth frame can be represented as [12]

$$P_{4b,m} = P[Re[X_{j,m}(n)Y^*_{j,m}(n)] < 0] = \frac{1}{2}\left[1 - \frac{\mu}{\sqrt{2-\mu^2}}\right], \tag{7}$$

where $P[a]$ and μ, respectively, denote the probability of a and the normalized covariance given as

$$\mu = \frac{Re[g_{xy}]}{\sqrt{g_{xx}g_{yy} - Im[g_{xy}]^2}}, \tag{8}$$

with $g_{xx} = E[|X_{j,m}(n)|^2]$, $g_{yy} = E[|Y_{j,m}(n)|^2]$, $g_{xy} = E[X_{j,m}(n)Y^*_{j,m}(n)]$

B. Second-order Moment Functions

In this subsection, we evaluate the impact of imperfect CSI with practical pilot-assisted CE scheme for broadband ANC [10] briefly explained in the previous section with different interpolation techniques.

1) First-order interpolation: The 1^{st} order interpolated channel gain $\bar{H}^k_{q,j,m}(n)$ at the mth block is obtained as

$$\begin{aligned}\bar{H}^k_{q,j,m}(n) &= \tfrac{M-m}{M}[H^k_{q,j,0}(n) + \epsilon^k_{q,j,0}(n)] \\ &+ \tfrac{m}{M}[H^{k+1}_{q,j,0}(n) + \epsilon^{k+1}_{q,j,0}(n)]\end{aligned} \tag{9}$$

for $n = 0 \sim N_c - 1$. Thus, the second-moment covariance functions for the first-order interpolation can be expressed as

$$\left\{\begin{aligned} g_{xx} &= 2\tfrac{P_s^2}{\beta^2} + (\tfrac{P_s}{\beta^2}+1)2\sigma_n^2 \\ &-2\tfrac{P_s^2}{\beta^2}\big[(\tfrac{M-m}{m})J_0(2\pi f_D T_s m) \\ &+(\tfrac{M}{m})J_0(2\pi f_D T_s(M-m))\big]^2 \\ &+\tfrac{P_s^2}{\beta^2}\big[(\tfrac{M-m}{m})^2 + (\tfrac{M}{m})^2\big]^2(1+2\sigma_e^2)^2 \\ &+4\tfrac{P_s^2}{\beta^2}(\tfrac{M-m}{m})^3(\tfrac{M}{m})(1+2\sigma_e^2)J_0(2\pi f_D T_s M) \\ &+4\tfrac{P_s^2}{\beta^2}(\tfrac{M-m}{m})(\tfrac{M}{m})^3(1+2\sigma_e^2)J_0(2\pi f_D T_s M) \\ &+4\tfrac{P_s^2}{\beta^2}(\tfrac{M-m}{m})^2(\tfrac{M}{m})^2 J_0^2(2\pi f_D T_s M) \\ &= 2\tfrac{P_s^2}{\beta^2} + (\tfrac{P_s}{\beta^2}+1)2\sigma_n^2 + \tfrac{P_s^2}{\beta^2}A_1 + \tfrac{P_s^2}{\beta^2}g_{yy}, \\ g_{yy} &= \big[(\tfrac{M-m}{m})^2 + (\tfrac{M}{m})^2\big]^2(1+2\sigma_e^2)^2 \\ &+4(\tfrac{M-m}{m})^3(\tfrac{M}{m})(1+2\sigma_e^2)J_0(2\pi f_D T_s M) \\ &+4(\tfrac{M-m}{m})(\tfrac{M}{m})^3(1+2\sigma_e^2)J_0(2\pi f_D T_s M) \\ &+4(\tfrac{M-m}{m})^2(\tfrac{M}{m})^2 J_0^2(2\pi f_D T_s M), \\ g_{xy} &= \tfrac{P_s}{\beta}\big[(\tfrac{M-m}{m})J_0(2\pi f_D T_s m) \\ &+(\tfrac{M}{m})J_0(2\pi f_D T_s(M-m))\big]^2 \\ &= \tfrac{P_s}{\beta}A_2, \end{aligned}\right. \tag{10}$$

where $J_0(\cdot)$ is the zeroth order Bessel function of first kind and f_D is the maximum Doppler shift. σ_e^2 is the variance of channel estimation error $\epsilon_{q,j,m}(n)$ and $\sigma_n^2 = N_0/T_s$ is the noise power due to AWGN with $1/T_s$ being data symbol rate. We note here that we assume the Jakes fading model, where incoming rays constituting each propagation path arrive at a user with uniformly distributed angles with the correlation given by $E[H^k_{q,j,m}(n)H^{k'}_{q',j,m}(n)] = J_0(2\pi f_D T_s(k-k')$ [11]. We also consider the block fading, where the fading gains remain constant during one time slot and vary slot-by-slot.

2) Second order interpolation: The 2^{nd} order interpolated channel gain $\bar{H}^k_{q,j,m}(n)$ at the mth block is obtained as

$$\begin{aligned}\bar{H}^k_{q,j,m}(n) &= \tfrac{(M-m)(m-2M)}{2M^2}[H^k_{q,j,0}(n) + \epsilon^k_{q,j,0}(n)] \\ &+ \tfrac{m(2M-m)}{M}[H^{k+1}_{q,j,0}(n) + \epsilon^{k+1}_{q,j,0}(n)] \\ &+ \tfrac{m(m-M)}{2M^2}[H^{k+2}_{q,j,0}(n) + \epsilon^{k+2}_{q,j,0}(n)]\end{aligned} \tag{11}$$

for $n = 0 \sim N_c - 1$. Thus, the second-moment covariance functions for the second-order interpolation are given by

$$\left\{\begin{aligned} & g_{xx} = 2\tfrac{P_s^2}{\beta^2} + (\tfrac{P_s}{\beta^2}+1)2\sigma_n^2 + 2\tfrac{m(m-M)(2M-m)^2}{M^4}\tfrac{P_s^2}{\beta^2} \\ & \times J_0(2\pi f_D T_s m)J_0(2\pi f_D T_s(M-m)) \\ & +\tfrac{P_s^2 m(m-M)^2(2M-m)}{\beta^2 M^4}J_0(2\pi f_D T_s m)J_0(2\pi f_D T_s(2M-m)) \\ & -\tfrac{2P_s^2 m^2(m-M)(2M-m)}{\beta^2 M^4}J_0(2\pi f_D T_s(M-m)) \\ & \times J_0(2\pi f_D T_s(2M-m)) - \tfrac{(m-M)^2(2M-m)^2}{2M^4}\tfrac{P_s^2}{\beta^2} \\ & \times J_0^2(2\pi f_D T_s m) - 2\tfrac{m^2(2M-m)^2}{M^4}\tfrac{P_s^2}{\beta^2}J_0^2(2\pi f_D T_s(M-m)) \\ & -\tfrac{m^2(m-M)^2}{2M^4}\tfrac{P_s^2}{\beta^2}J_0^2(2\pi f_D T_s(2M-m)) + \tfrac{P_s^2}{\beta^2}g_{yy} \\ & = 2\tfrac{P_s^2}{\beta^2} + (\tfrac{P_s}{\beta^2}+1)2\sigma_n^2 + \tfrac{P_s^2}{\beta^2}A_1 + \tfrac{P_s^2}{\beta^2}g_{yy}, \\ & g_{yy} = \big[(\tfrac{(M-m)^4(2M-m)^4}{16M^8} + \tfrac{m^4(2M-m)^4}{M^8} + \tfrac{m^4(m-M)^4}{16M^8} \\ & +\tfrac{m^2(m-M)^4(2M-m)^2}{8M^8} + \tfrac{m^4(m-M)^2(2M-m)^2}{2M^8} \\ & +\tfrac{m^2(m-M)^2(2M-m)^4}{2M^8}\big](1+2\sigma_e^2)^2 + \big[\tfrac{m^2(m-M)^2(2M-m)^4}{M^8} \\ & +\tfrac{m^4(m-M)^2(2M-m)^2}{M^8} - 2\tfrac{m^3(m-M)^2(2M-m)^3}{M^8}\big] \\ & \times J_0^2(2\pi f_D T_s M) + \tfrac{m^2(m-M)^4(2M-m)^2}{4M^8}J_0^2(2\pi f_D T_s 2M) \\ & +\big[\tfrac{m^2(m-M)^3(2M-m)^3}{M^8} - \tfrac{m^3(m-M)^3(2M-m)^2}{M^8}\big] \\ & \times J_0^2(2\pi f_D T_s M)J_0^2(2\pi f_D T_s 2M) \\ & +\big[2\tfrac{m^4(m-M)(2M-m)^3}{M^8} - \tfrac{m(m-M)^3(2M-m)^4}{2M^8} \\ & -2\tfrac{m^3(m-M)(2M-m)^4}{M^8} + \tfrac{m^4(m-M)^3(2M-m)}{2M^8} \\ & +\tfrac{m^2(m-M)^3(2M-m)^3}{2M^8} - \tfrac{m^3(m-M)^3(2M-m)^2}{2M^8}\big](1+2\sigma_e^2) \\ & \times J_0(2\pi f_D T_s M) - \big[\tfrac{m(m-M)^4(2M-m)^3}{4M^8} \\ & +\tfrac{m^3(m-M)^2(2M-m)^3}{M^8} + \tfrac{m^3(m-M)^4(2M-m)}{4M^8}\big](1+2\sigma_e^2) \\ & \times J_0(2\pi f_D T_s 2M), \\ & g_{xy} = \tfrac{(m-M)^2(2M-m)^2}{4M^4}\tfrac{P_s}{\beta}J_0^2(2\pi f_D T_s m) + \tfrac{P_s m^2(2M-m)^2}{\beta M^4} \\ & \times J_0^2(2\pi f_D T_s(M-m)) + \tfrac{m^2(m-M)^2}{4M^4}\tfrac{P_s}{\beta} \\ & \times J_0^2(2\pi f_D T_s(2M-m)) - \tfrac{m(m-M)(2M-m)^2}{M^4}\tfrac{P_s}{\beta} \\ & \times J_0(2\pi f_D T_s m)J_0(2\pi f_D T_s(M-m)) \\ & -\tfrac{P_s m(m-M)^2(2M-m)}{2\beta M^4} \\ & \times J_0(2\pi f_D T_s m)J_0(2\pi f_D T_s(2M-m)) \\ & +\tfrac{m^2(m-M)(2M-m)}{M^4}\tfrac{P_s}{\beta}J_0(2\pi f_D T_s(M-m)) \\ & \times J_0(2\pi f_D T_s(2M-m)) \\ & = \tfrac{P_s}{\beta}A_2. \end{aligned}\right. \tag{12}$$

3) BER Evaluation: Using the second moment covariance functions for practical pilot-assisted CE with both the first and second order interpolation we obtain the normalized covariance as

$$\mu = \frac{A_2}{\sqrt{(2+(\frac{E_s}{2N_0})^{-1} + (\frac{E_s}{2N_0})^{-2} + A_1 + g_{yy})g_{yy}}}. \tag{13}$$

TABLE I
NUMERICAL SIMULATION PARAMETERS.

Tx	Data modulation	QPSK
	Block size	$N_c = 256$
	GI	$N_g = 32$
Channel	L-path block Rayleigh fading channel	
Rx	Equalization	MRC

Thus, the BER performance for broadband ANC with first and second order interpolation schemes is finally derived as

$$P_{4b,m} = \frac{1}{2}\left[1 - \frac{A_2}{\sqrt{(4+2(\frac{E_s}{2N_0})^{-1}+2(\frac{E_s}{2N_0})^{-2}+2A_1+2g_{yy})g_{yy}-A_2^2}}\right]. \quad (14)$$

The average BER expression for the OFDM frame is finally calculated by averaging the $M-1$ data blocks as

$$P_{4b} = \sum_{m=1}^{M-1} P_{4b,m}. \quad (15)$$

Next a closed-form BER for broadband ANC with perfect knowledge of CSI is given as a reference.

C. BER with perfect CSI

In the case of perfect knowledge of CSI the second moments are given by $g_{xx} = P^2/\beta^2 + (P/\beta^2 + 1)2\sigma_n^2$, $g_{yy} = 1$ and $g_{xy} = P/\beta$. Thus, the average BER is obtained by

$$P_{4b} = \frac{1}{2}\left[1 - \frac{1}{\sqrt{1+2(\frac{E_s}{2N_0})^{-1}+2(\frac{E_s}{2N_0})^{-2}}}\right]. \quad (16)$$

Next we present the numerical results and discussions based on the analysis presented in the this section.

IV. NUMERICAL RESULTS

The numerical simulation parameters are shown in Table I. We assume ideal coherent QPSK modulation/demodulation with $N_c = 256$ and GI length of $N_g = 32$. The propagation channel is an L-path Rayleigh fading channel, where the path gains $\{h_{q,l,j,m}; l = 0 \sim L-1\}$ are zero-mean independent complex variables with $E[|h_{q,l,j,m}|^2] = 1/L$. The maximum time delay of the channel is assumed to be less than the guard interval and that all paths are independent of each other. $f_D T_s$ denotes the normalized Doppler frequency, where $1/T_s$ is the transmission symbol rate ($f_D T_s = 10^{-3}$ corresponds to a mobile terminal speed of approximately 83 km/h for a transmission data rate of 100 Msymbols/s and a carrier frequency of 5GHz). Distance-dependent path loss and shadowing loss are not considered.

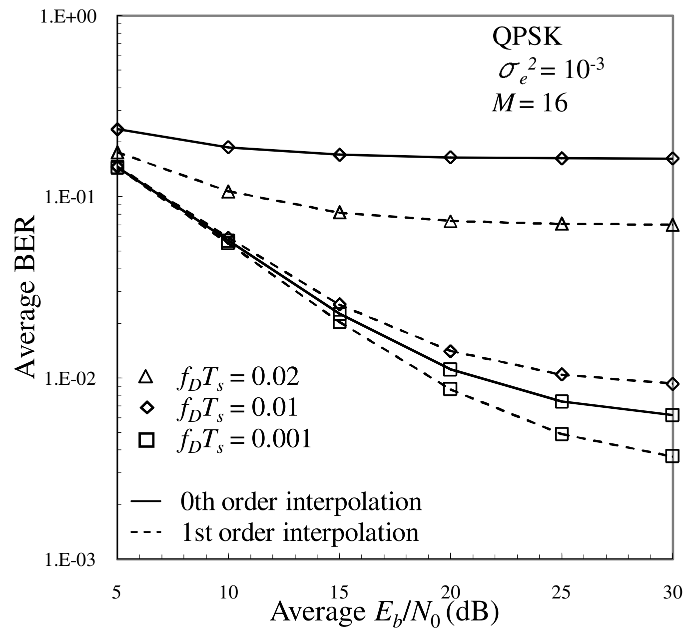

Fig. 3. BER performance using 1^{st} order interpolation.

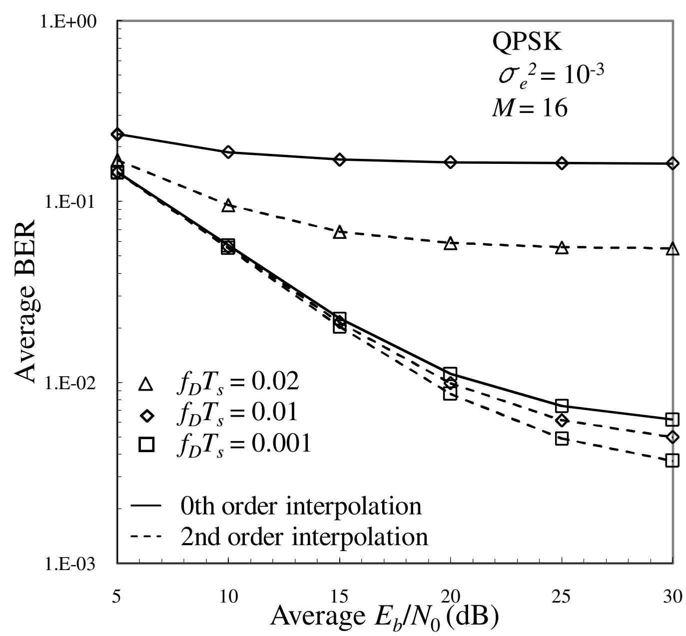

Fig. 4. BER performance using 2^{nd} order interpolation.

Figure 3 shows the BER performance of broadband ANC using pilot-assisted CE with the first-order interpolation as a function of E_b/N_0 with $f_D T_s$ as a parameter with $\sigma_e^2 = 10^{-3}$ and $M = 16$. The tracking ability is noticeable improved for pilot-assisted CE with the first-order interpolation in comparison to the case without interpolation (i.e., 0^{th} order). The figure shows that pilot-assisted CE scheme with the first-order interpolation slightly improves the BER perfomance for the mobile user veocity of about 80 km/h (corresponds to the normalized Doppler frequency $f_D T_s = 10^{-3}$). On the other hand, for the mobile user velocity of about 800 km/h (corresponds to the normalized Doppler frequency $f_D T_s = 10^{-2}$) the significant BER performance improvement is observed in comparison with the CE case where interpolation is not used. However, for a higher mobile user velocity (corresponding to the normalized Doppler frequency $f_D T_s = 10^{-1}$) a BER floor is observed due to a fast fading variation that cannot be tracked by the first-order interpolation.

Figure 4 shows the BER performance of broadband ANC using pilot-assisted CE with the second-order interpolation as a function of E_b/N_0 with $f_D T_s$ as a parameter. The values of σ_e^2 and M are same as in Fig. 3. For the the mobile user speed of about 80 km/h (i.e., normalized Doppler frequency $f_D T_s = 10^{-3}$) the second-order interpolation slightly improves the BER performance in comparison with the CE case when interpolation is not used (i.e., 0^{th} order). The larger BER performance gain with the second-order interpolation can be observed for the mobile user velocity of about 800 km/h (i.e., normalized Doppler frequency $f_D T_s = 10^{-2}$), while for the higher velocity (corresponding to the normalized Doppler frequency $f_D T_s = 10^{-1}$) the BER performance severely degrades since the channel fluctuations are too fast and they cannot be encountered by the polynomial interpolation.

V. Conclusion

In this paper, we presented the closed-form BER expressions for bi-directional ANC with practical pilot-assisted CE scheme in a frequency-selective fading channel. As a physical layer access we consider OFDM radio. We evaluate the impact of the first and second order time domain interpolation on the practical pilot-assisted CE scheme on the achievable BER performance of bi-directional ANC with OFDM. It was shown that the BER performance gains in a higher E_b/N_0 region for both the first and second-order polynomial time-domain channel interpolation depend on a mobile user velocity. Further performance improvements can be obtained by using a higher order interpolation techniques, but their analysis may become very difficult if not impossible to track.

Acknowledgment

This work was supported in part by 2010 KDDI Research Grant Program.

References

[1] P. Popovski and H. Yomo, "Bi-directional amplification of throughput in a wireless multi-hop network," the IEEE 63^{rd} Vehicular Technology Conference (VTC), Melbourne, Australia, May 2006.

[2] S. Zhang, S.-C. Liew, and P. Lam, "Hot topic: Physical layer network coding," ACM The 12^{th} MobiCom 2006, pp. 358-365, 23-26 September 2006, Los Angelos, USA.

[3] S. Katti, S. S. Gollakota, and D. Katabi, "Embracing wireless interference: Analog network coding," ACM SIGCOM 2007, Kyoto, Japan, 27-21 August, 2007.

[4] S. Zhang, S. C. Liew and L. Lu, "Physical layer network schemes over finite and infinite fields," The 2008 Global Communications Conference (Globecom 2008), 30. Nov.-4. Dec. 2008, New Orleans, USA.

[5] P. Larsson, N. Johansson and K.-E. Sunell, "Coded bi-directional relaying," The 2006 Vehicular Technology Conference (VTC 2006-Spring), pp. 851-855, May 2006, Melburn, Australia.

[6] K. Narayanan, M. P. Wilson and A. Sprintson, "Joint physical layer coding and network coding for bi-directional relaying," 45th Allerton Conference on Communication, Control, and Computing, September 26-28, 2007, Ilinois, USA.

[7] Y.-C. Liang and R. Zhang, "Optimal analogue relaying with multi-antennas for physical layer network coding," The 2008 IEEE International Conference on Communications (ICC'08), 19-23 May 2008, Beijing, China.

[8] H. Gacanin and F. Adachi, "Broadband analog network coding," IEEE Trans. on Wireless Communications, Vol. 9, No. 5, pp. 1577-1583, May 2010.

[9] F. Gao, R. Zhang, and Y-C. Liang, "On Channel Estimation for Amplify-and-Forward Two-Way Relay Networks", the 2008 IEEE Global Communication Conference (Globecom'08), New Orleans, LA, USA, December 2008.

[10] T. Sjodin, H. Gacanin, and F. Adachi, "Two-slot Channel Estimation for Analog Network Coding Based on OFDM in a Frequency-selective Fading Channel", the 2010 IEEE 71^{th} Vehicular Technology Conference (VTC2010-Spring), 16-19 May 2010, Taipei, Taiwan.

[11] W. C. Jakes, Microwave Mobile Communications, 2nd ed., IEEE Press, 1993.

[12] J. G. Proakis, Digital communications, 3rd ed., McGraw-Hill, 1995.